JOURNAL OF THE
ANUS, RECTUM AND COLON
dx.doi.org/10.23922/jarc.2024-014
http://journal-arc.jp

Original Research Article

Reduced Abundance of *Phocaeicola* in Mucosa-associated Microbiota Is Associated with Distal Colorectal Cancer Metastases Possibly through an Altered Local Immune Environment

Gaku Ota[1)], Ryo Inoue[2)], Akira Saito[1)], Yoshihiko Kono[1)], Joji Kitayama[1)3)], Naohiro Sata[1)] and Hisanaga Horie[1)4)]

1) Department of Surgery, Jichi Medical University, Shimotsuke, Japan
2) Laboratory of Animal Science, Department of Applied Biological Sciences, Faculty of Agriculture, Setsunan University, Hirakata, Japan
3) Clinical Research Center, Division of Translational Research, Jichi Medical University, Shimotsuke, Japan
4) Department of Operating Room Management, Jichi Medical University Hospital, Shimotsuke, Japan

Abstract

Objectives: The aim of this study was to identify the microbiota whose decrease in tumor area was associated with the metastatic process of distal colorectal cancer (CRC).

Methods: Twenty-eight consecutive patients with distal CRC undergoing surgical resection in our hospital were enrolled. Microbiota in 28 specimens from surgically resected colorectal cancers were analyzed using 16S ribosomal ribonucleic acid gene amplicon sequencing and the relative abundance (RA) of microbiota was evaluated. The densities of tumor-infiltrating lymphocytes (TIL) and tumor associated macrophages (TAM) in the colorectal cancers were immunohistochemically evaluated.

Results: *Phocaeicola* was the most abundant microbiota in normal mucosa. The RA of *Phocaeicola* in tumor tissues tended to be lower than that in normal mucosa although the difference was not significant ($p=0.0732$). The RA of *Phocaeicola* at tumor sites did not correlate either with depth of tumor invasion (pT-stage) or tumor size, however they were significantly reduced in patients with nodal metastases ($p<0.05$) and those with distant metastases ($p<0.001$). The RA of *Phocaeicola* at tumor sites showed positive correlation with the densities of CD3(+) or CD8(+) TIL. Since *P. vulgatus* was the most dominant species (47%) of the *Phocaeicola*, the RA of *P. vulgatus* and CRC metastasis and its association with TIL and TAM were also investigated. *P. vulgatus* showed a similar trend to genus *Phocaeicola* but was not statistically significant.

Conclusions: A relative reduction of *Phocaeicola* attenuates the local anti-tumor immune response in distal CRC, which may facilitate metastatic spread.

Keywords

Phocaeicola, colorectal cancer, tumor infiltrating lymphocytes, tumor associated macrophage

J Anus Rectum Colon 2024; 8(3): 235-245

Introduction

Research on the association between dysbiosis and colorectal cancer (CRC) has focused on intestinal microbiota that increase in fecal samples of CRC patients or mucosal samples of the tumor surface. Increased abundance of *Fusobacterium nucleatum*[1-5], *Parvimonas micra*[3,4,6] and some species of *Peptostreptococcus*[2-6], *Streptpcoccus*[5,7]

Corresponding author: Gaku Ota, goatkau@jichi.ac.jp
Received: March 1, 2024, Accepted: May 17, 2024

were reported. We also reported significant increase of *Fusobacterium* and *Streptococcus* in the mucosal samples of tumor from CRC patients[8]. Therefore, it is speculated that microbiota listed above are involved in colon carcinogenesis. On the other hand, it has been reported that *Phocaeicola vulgatus* and *Phocaeicola dorei* (changed from *Bacteriodes vulgatus* and *dorei* in 2019[9]) in fecal samples decreased in patients with coronary artery disease compared to healthy subjects[10,11]. The mechanism by which *P. vulgatus* prevents coronary artery disease is also under investigation[11]. Therefore, when studying dysbiosis even in patients with colorectal cancer, it may be useful to focus on decreased intestinal microbiota in the tumor area and analyze its relationship with tumor development and progression, as this may lead to new findings.

It has also been reported that local immune responses around tumors are involved in the development and progression of solid tumors. Recent studies have shown that the degree of infiltration of different types of immune cells and their distribution patterns are significantly associated with tumor progression[12,13] and clinical outcomes, especially patients treated with immunotherapy[14,15]. In general, infiltration of CD3(+) T lymphocytes (tumor-infiltrating lymphocytes: TIL), especially CD8(+) cytotoxic T cells, into solid tumors is associated with a good prognosis for patients with various types of cancer including CRC[14-17]. Another important cell type infiltrating tumor tissue is the macrophage. Tumor-associated macrophages (TAM) are known to be generally polarized to the immunosuppressive M2 phenotype and facilitate a protumorigenic function by producing anti-inflammatory cytokines or angiogenic factors[13,18]. However, the relationship between immune cells infiltrating the tumor and the microbiome in CRC is not clearly understood.

In the present study, we reanalyzed the relative abundance (RA) of gut microbiome from CRC patients previously reported by us[8] to search for intestinal microbiota whose decrease in the tumor area was associated with metastasis. Then, the correlation between the RA of microbiota in tumors with tumor immune cell populations detected by immunohistochemistry (IHC) was examined to gain insight into the mechanism of the involvement of microbiota in the metastatic spread of CRC. As stated in the previous paper, there are many biological differences between proximal and distal CRCs and the incidence of CRC in the distal large intestine is higher than that in the proximal large intestine. Therefore, we focused on distal CRC in this study.

Methods

Patients

In total, 28 consecutive patients with distal CRC and histologically confirmed adenocarcinoma undergoing surgical resection at the Department of Surgery of Jichi Medical University between June 2018 and April 2019 were recruited. Patients with colorectal tumors other than adenocarcinoma, who had adenocarcinoma in the cecum, ascending colon, transverse colon, or descending colon, who received preoperative chemotherapy or radiotherapy, who received antibiotics before operation, or who had comorbid malignancies associated with other organs were excluded. This study was approved by the Institutional Review Board of Jichi Medical University Hospital (approval number: A17-083) and was conducted in accordance with the guiding principles of the Declaration of Helsinki, and written informed consent was obtained from each patient before inclusion in the study.

Sample collection, DNA extraction, data analysis and taxonomy assignment

In this study, the RA of the microbiota in the tumor and the RA in normal mucosa 6 cm away from the tumor in the previous study[8] were used for analysis, which also describes the methods of sample collection, DNA extraction and data analysis, and taxonomy assignment. In brief, tissue samples were collected from resected specimens in the operating room. After removal of the sigmoid colon or rectum, the intestine was cut longitudinally and opened on a clean bench. The mucosal surface of the intestine was gently washed with sterile saline and any residual feces on the mucosal surface removed. Tissue samples measuring 3×3 mm were collected from the tumor as well as normal mucosa. To avoid contamination, one sterile knife and forceps were used to harvest one sample. Each sample was placed in RNAlater (Life Technologies, Tokyo, Japan) separately at 4°C for 24hrs and then stored at -80°C until processing. Genomic DNA was isolated from the samples using the QuickGene DNA tissue kit (KURABO, Osaka, Japan) as previously described[19]. Library preparation including amplification by PCR of the V3-V4 region of the 16S rRNA gene was carried out exactly as previously described[20]. Deep sequencing was conducted using a MiSeq System (Illumina, Tokyo, Japan). Generation of the amplicon sequence variant (ASV) table, including quality filtering and chimeric variant filtering was performed using Quantitative Insights Into Microbial Ecology 2 (QIIME2) version 2023.2 and the DADA2 plugin of QIIME2[21,22]. The taxonomy of each ASV was assigned by the Sklearn classifier algorithm against Greengenes2 database[23]. The ASVs classified into mitochondria and ASVs of phyla not assigned were removed to avoid contamination of host DNA.

Antibodies and reagents

Monoclonal antibodies (mAbs) to CD3 (60347-1-lg, clone 2E9G7) and CD8α (66868-1-lg, clone 1G2B10) were pur-

Table 1. Characteristics of Patients with Distal Colorectal Cancers (n=28).

Age (years)	Mean (range)	67 (42-85)
Gender	Male	21
	Female	7
Tumor location	Sigmoid colon	9
	Rectum	19
Tumor size	median (range)	31.5 mm (15-135)
Depth of tumor invasion	T1	8
	T2	4
	T3	13
	T4	3
Venous invasion	Negative	9
	Positive	19
Lymphatic invasion	Negative	19
	Positive	9
Histological type	Well	7
	Moderately	21
Nodal metastases	N0	20
	N1	5
	N2	3
Distant metastases	M0	25
	M1	3
Tumor stage	I	11
	II	9
	III	5
	IV	3

T1: Tumor is confined to the submucosa; T2: Tumor is confined to the muscularis propria; T3: Tumor invades beyond the muscularis propria; T4: Tumor invades or perforates the serosa or directly invades other organs or structures, Well: Well differentiated adenocarcinoma; Moderately: Moderately differentiated adenocarcinoma

chased from Proteintech Group (Rosemont, USA), and to CD68 (ab955, clone KP1) and CD163 (ab156769, clone OTI2G12) from Abcam (Cambridge, MA). Signal enhancer HIKARI for Immunostain Solution B, antibody dilution buffer, HistoVT One (10×, pH 7.0, 06380-05) and blocking solution One Histo (06349-64) were purchased from Nacalai Tesuque (Kyoto, Japan).

Histopathology and immunohistochemistry

Surgically resected specimens were fixed in formalin, embedded in paraffin, cut into 4-μm thick sections, and used for immunohistochemistry (IHC) analysis as well as hematoxylin & eosin staining. IHC staining was performed using the DAKO REAL™ Envision™ Detection system (Glostrup, Denmark). Briefly, after deparaffinization in xylene and rehydration in a graded series of ethanol baths, sections were washed with distilled water for 10 min. For antigen retrieval, the sections were processed by heating at 90°C in HistoVT One for 30 min. Endogenous peroxidases were blocked using 0.3% hydrogen peroxide for 30 min. After washing in phosphate-buffered saline (PBS), a nonspecific staining blocking agent (Blocking One Histo) was used to prevent nonspecific binding for 10 min. Sections were then incubated with primary antibodies to CD3 (1:100 dilution), CD8 α (1:4000), CD20 (1:1000), CD68 (1:200), and CD163 (1:300) for 60 min at room temperature. Sections were then thoroughly washed with PBS and incubated with DAKO REAL™ Envision™/HRP, Rabbit/Mouse (code K5007, DakoCytomation, Denmark), and primary antibody binding visualized using the DAKO Envision kit according to the manufacturer's instructions and counterstained with Meyer's hematoxylin.

To evaluate the density of immune cells, positive cells were counted in four randomly selected low magnification fields at the invasive front area under ×400 magnification in a light microscope. Analyses were blindly performed with respect to clinical outcomes by 2 investigators.

Statistical analysis

The RA of bacteria in the microbiota between groups was

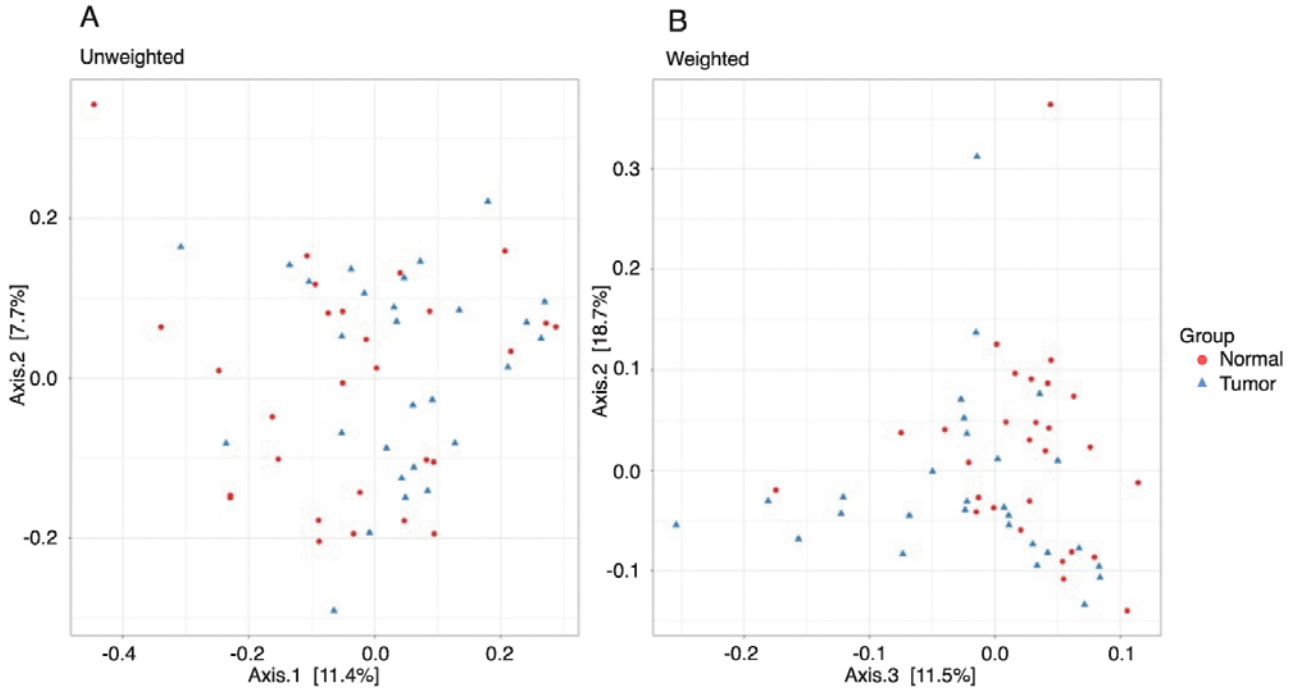

Figure 1. A: Principal coordinate analysis (PCoA) of microbiota variation in samples from tumor and normal mucosa in 28 patients with CRC based on unweighted UniFrac distances metrics. B: PCoA of microbiota variation in same samples based on weighted UniFrac distances metrics.

Table 2. Alpha-Diversity Indices.

	Tumor	Normal mucosa	p value
Chao 1 index median (min-max)	84.50 (15.00-240.75)	67.67 (15.00-236.00)	p>0.1
Shannon index median (min-max)	3.408 (1.503-4.476)	3.084 (2.200-4.307)	p>0.1

min: minimum, max: maximum

statistically compared by Mann-Whitney's U-test and the relationship between the RA of each microbe was analyzed using Spearman's correlation. The alpha-diversity indices (Chao 1 and Shannon phylogenetic diversity indices) were calculated by phyloseq package for R software and analyzed using Mann-Whitney's U-test. The beta-diversity based on the UniFrac distance was estimated by QIIME2 to calculate the distances between the samples and visualized by principal coordinate analysis (PCoA), and statistically examined using permutational multivariate analysis of variance (PERMANOVA). Statistical differences in clinical and pathological factors were evaluated with the Mann-Whitney's U-test and Kruskal-Wallis rank sum analysis. Correlations between immune cell densities and the RA of bacteria were analyzed with Spearman's rank correlation coefficients. Differences were considered significant when $p<0.05$.

Results

Reduced RA of Phocaeicola correlated with metastases in CRC

The characteristics of the 28 patients with CRC are shown in Table 1. Initially, the overall structure of the gut microbiome in samples from tumor and normal mucosa in these patients was calculated for unweighted and weighted UniFrac distances (Figure 1A, B). PCoA revealed that there were not microbial structural differences between tumor and normal mucosa in unweighted (PERMANOVA, $p>0.05$) and weighted (PERMANOVA, $p>0.05$) distances. The diversity of gut microbiota was evaluated using different alpha-diversity indices: the Chao 1 index and the Shannon index (Table 2). These alpha-diversity indices showed no statistically significant differences between tumor and normal mucosa.

Then, the difference in the gut microbial structure in tumor and normal mucosa were evaluated at the phylum level (Figure 2A). RAs of *Bacteroidota* were lower in tumor than normal mucosa. RA of *Fusobacteriota* were higher in tumor than normal mucosa. At the genus level (Figure 2B), *Bacteroides* were most abundant microbiota in tumor and *Phocaeicola* in normal mucosa. RA of *Fusobacterium*, *Streptococcus*, and *Peptostreptococcus* were higher in tumors than in normal tissues as shown in a previous report[8]. On the other hands, the RA of *Phocaeicola* tended to be lower in

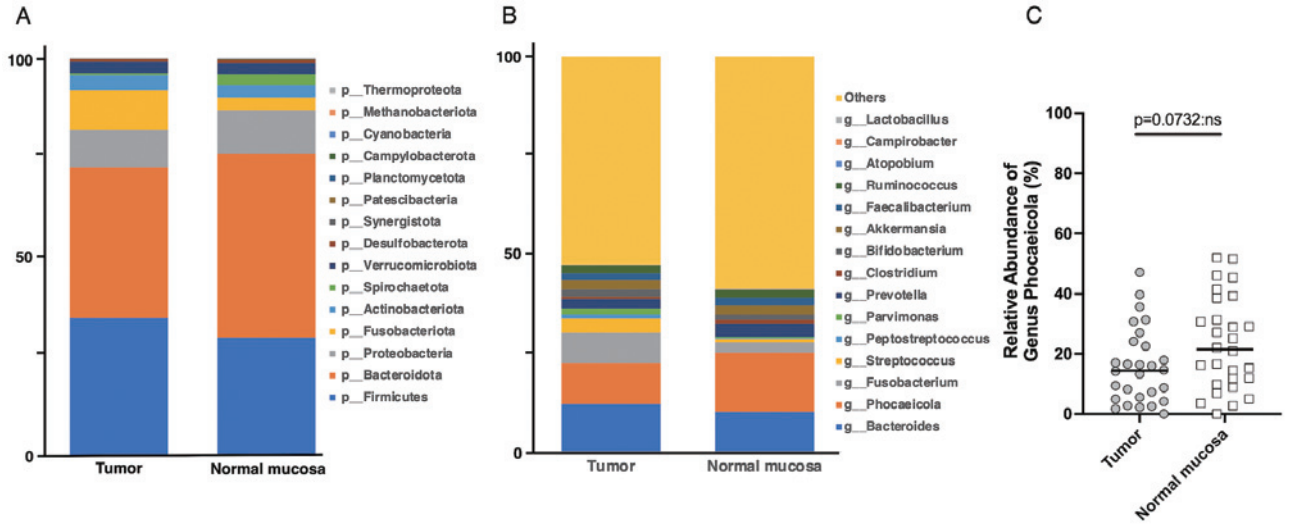

Figure 2. A: Average of Relative abundance (RA) of microbiome genes at the phylum level in surgical specimens derived from tumor and corresponding normal mucosa in 28 patients with CRC. B: Average of RA of microbiome genes at the genus level in same specimens. C: The RA of genus *Phocaeicola* in tumor and normal mucosa in each patient. P-value was evaluated using the Mann-Whitney U-test.

tumor tissues although the difference was not significant (p= 0.0732) (Figure 2C).

As shown in Figure 3A, B, the RAs of *Phocaeicola* in tumor sites were not affected either by depth of tumor invasion (pT-stage) or length of tumor major axis (mm). However, the RAs of *Phocaeicola* were significantly lower in patients with nodal involvement than those without nodal metastases (p=0.0114) and significantly lower in tumors with distant metastases (p=0.0098, Figure 3C, D). On the other hand, the association between the RA and pathological factors such as tumor grade (Figure 3E), budding (Figure 3F), lymphatic invasion (Figure 3G), and venous invasion (Figure 3H) was not statistically significant, although it was lower in tumors with high tumor grade or budding grade, tumors with lymphatic invasion, and tumors with venous invasion.

Densities of TIL and TAM correlated with nodal and distant metastases from CRC

We next examined the phenotypes of T cells (TILs) and macrophages (TAM) infiltrating resected CRC tumors using IHC with specific mAbs to CD3, CD8 and CD68, CD163, respectively (Figure 4A, B). As shown in Figure 5A-a, d, the densities of CD3(+) TILs were significantly less in CRC with nodal (p=0.002) or distant metastases (p=0.006) than those without metastases. The densities of CD8(+) TILs were reduced more prominently (p<0.001, p=0.002 in Figure 5A-b, e), and CD8/CD3 ratios were decreased in tissue from patients with metastatic CRC (p=0.004, p=0.04 in Figure 5 A-c, f). The densities of CD68(+) TAMs in CRC did not differ in tissue from patients with metastatic and non-metastatic tumors (Figure 5B-a, d). However, CD163(+) TAMs with M2 phenotype were significantly increased (p= 0.011) and the ratios against CD68(+) total macrophages were higher (p<0.001) in tumors from patients with lymph node metastases (Figure 5B-b, c). Similar trends were observed in tissue from patients with distant metastases, although the difference was not statistically significant (p= 0.090, p=0.13 in Figure 5B-e, f).

RAs of Phocaeicola correlated with the densities of TILs

As shown in Figure 6A, B, the densities of CD3(+) and CD8(+) TILs had positive correlations with the RAs of *Phocaeicola* (CD3 r=0.4987, p=0.0069; CD8 r=0.5116, p= 0.0054). However, CD8/CD3 ratios did not correlate with the RAs of *Phocaeicola* (Figure 6C). On the other hand, there were no correlations between the RAs of *Phocaeicola* and the densities of CD68(+) TAMs, CD163(+) TAMs, or CD163/CD68 ratios (Figure 6D, E, F).

Species-level analysis of the genus Phocaeicola

Next, the nearest known species of ASVs belonging to genus *Phocaeicola* were identified. In total, 123 ASVs belonged to the *Phocaeicola*. Fifty-eight of the 123 ASVs (47%) showed the highest similarity to *P. vulgatus*, 19 ASVs to *P. dorei*, 19 ASVs to *P. massiliensis*, 14 ASVs to *P. plebeius*, 7 ASVs to *P. coprocola*, 2 ASVs to *P. coprophilus*, 1 ASVs to *P. sartorii*, and 3 ASVs could not be classified to a specific species. Since *P. vulgatus* was the most dominant species, the RA of *P. vulgatus* and CRC metastasis and its association with TIL and TAM were investigated. *P. vulgatus* showed a similar trend to genus *Phocaeicola* but was not statistically significant (Supplementary Figure S1).

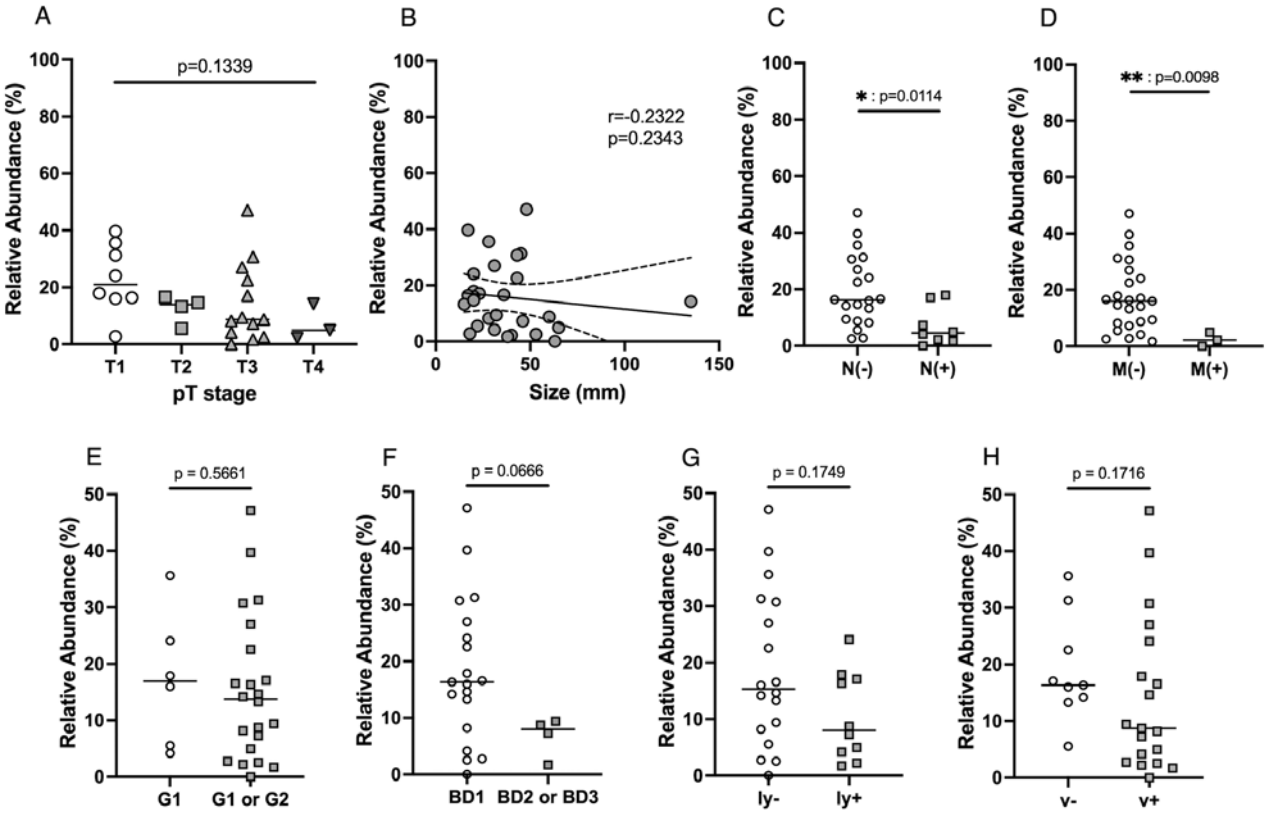

Figure 3. Correlations of relative abundance (RA) of *Phocaeicola* with pT stage (A), tumor diameter (B), pN stage (C), pM stage (D), tumor grade (E), tumor budding (F), lymphatic invasion (G), and venous invasion (H). Differences among pT stage were analyzed using the Kruskal-Wallis test and between pN, pM stages, tumor grade, tumor budding, lymphatic invasion, and venous invasion using the Mann-Whitney U-test. N: lymph node metastases, M: distant metastases, G1: papillary adenocarcinoma and well-differentiated tubular adenocarcinoma, G2: moderately differentiated adenocarcinoma, G3: poorly differentiated adenocarcinoma, mucinous adenocarcinoma, or signet ring cell carcinoma. Tumor budding was defined as a cancer cell nest consisting of 1 or <5 cells that infiltrated the interstitium at the invasive margin of the cancer and was graded according to its number in a microscopic field with a 20X objective lens (.785 mm^2) in the hotspot. Tumor budding was graded based on the number of buds as BD1 (<5), BD2 (5-9), or BD3 (>10). Correlations with tumor size were evaluated with Spearman's rank correlation coefficients tests. *: $p<0.05$, **: $p<0.01$.

Discussion

Phocaeicola, a genus of Gram-negative, are abundant everywhere in the human gut. In this study, the RAs of *Phocaeicola* were relatively low in tumor tissue compared with normal counterparts. The decrease of *Phocaeicola* in the tumor area may simply be a relative change due to an increase of CRC-linked microbiota such as *Fusobacterium*, *Streptococcus*, and *Peptostreptococcus*. However, the RA of *Phocaeicola* in CRC tissues was significantly reduced in tumors from patients with nodal metastases, and those with distant metastases. Therefore, the decrease of *Phocaeicola* in the tumor area was assumed to be related to the metastasis of colon cancer.

The results of IHC showed that TILs which associate with a good prognosis had low infiltration in patients with lymph node metastases or distant metastases; conversely, M2-type macrophages which has immunosuppressive function had high infiltration in patients with lymph node metastases or distant metastases (Figure 5). These results were mostly consistent with the results from previous studies[14,16,24,25].

The densities of CD3(+) and CD8(+) TILs had positive correlations with the RAs of *Phocaeicola* (Figure 6). A similar trend was observed for CD8/CD3, but not significant. Therefore, the RA of *Phocaeicola* seems to influence the degree of TIL infiltration into the tumor. On the other hand, there were no correlations between the RAs of *Phocaeicola* and the densities of CD68(+) TAMs, CD163(+) TAMs, or CD163/CD68 ratios. Therefore, the RA of *Phocaeicola* did not appear to affect infiltration of TAMs. These results showed that reduced RA of *Phocaeicola*, one of the most predominant anaerobes in the gut, was significantly associated with infiltration of TIL as well as metastatic status.

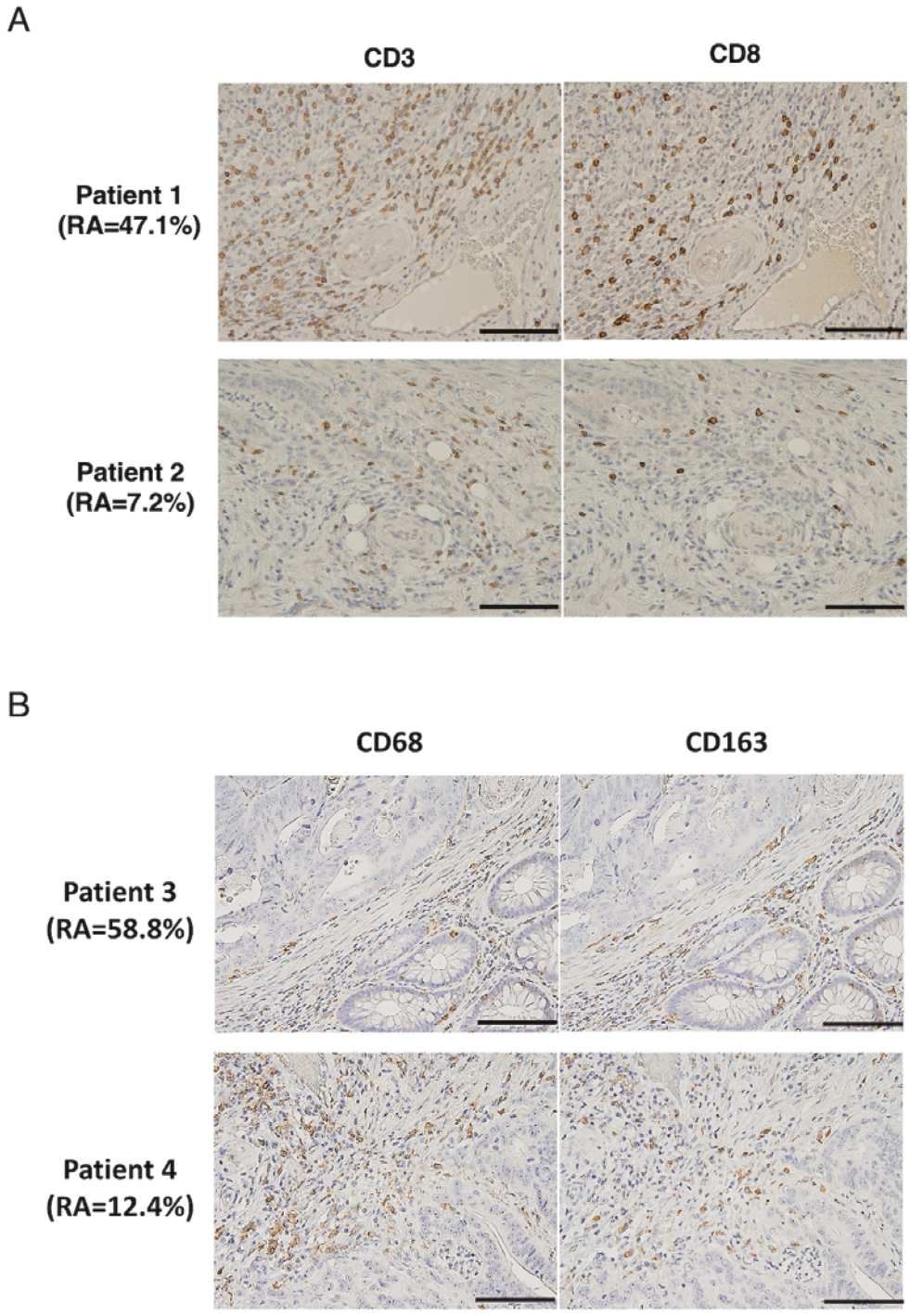

Figure 4. A: Immunostaining of tumor-infiltrating lymphocytes (TIL) at the invasive front area in colorectal tumor tissue of 2 representative patients with high (47.1%) and low (7.2%) relative abundance of *Phocaeicola*. Black bars show 100 μm. B: Immunostaining of tumor-associated macrophages (TAM) at the invasive front area in colorectal tumor tissue of 2 representative patients with high (58.8%) and low (12.4%) relative abundance of *Phocaeicola*. Black bars show 100 μm.

It has been reported that increased TIL in the tumor microenvironment, especially CD8(+) TILs, was associated with suppression of metastasis[26,27]. It is suggested that mechanisms via TIL infiltration may be involved in the RA of *Phocaeicola* being associated only with metastasis.

The mechanism of how *Phocaeicola* affects lymphocytes and macrophages remains unclear. Tryptophan metabolites derived from intestinal microbiota have been reported to induce immunosuppression by activating the aryl hydrocarbon receptor (AhR)[28]. It was also reported that AhR regulated

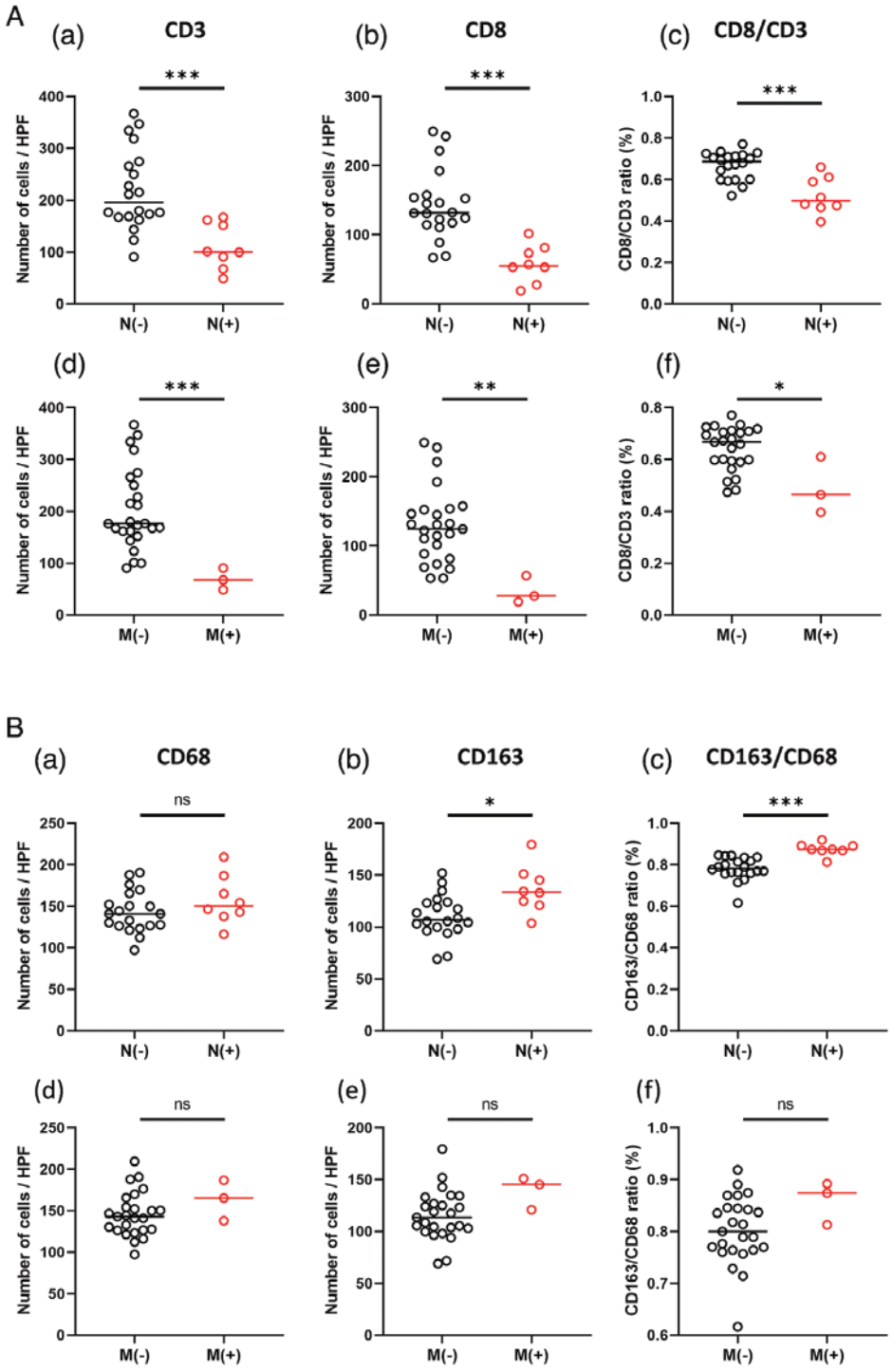

Figure 5. A: The densities of CD3(+) (a, d) and CD8(+) (b, e) tumor infiltrating lymphocytes (TIL) and CD8/CD3 ratios (c, f) in 28 colorectal cancers (CRC) with or without nodal (upper panel) or distant (lower panel) metastases. N: lymph node metastases, M: distant metastases. Positive cells were counted at 4 randomly selected fields in the invasive front area. B: The densities of tumor associated macrophages (TAM) in 28 colorectal cancers (CRC) with or without nodal (upper panel) or distant (lower panel) metastases. N: lymph node metastases, M: distant metastases. The whole TAM (a, d) and M2 type TAM (b, e) were determined as CD68(+) and CD163(+) cells, respectively, and counted at 4 randomly selected fields in the invasive front area. HPF= High power field, Differences were evaluated with the Mann-Whitney U-test. *: $p<0.05$, **: $p<0.01$, ***: $p<0.001$.

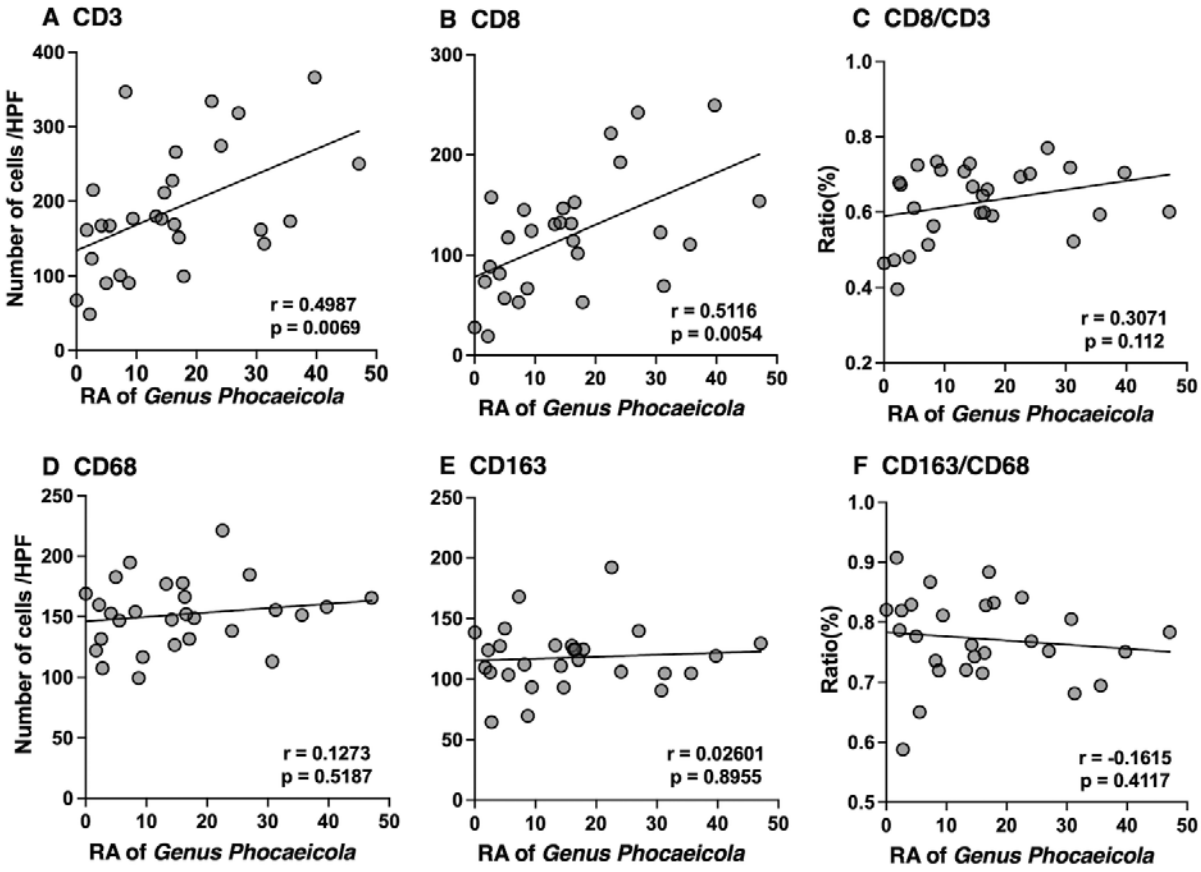

Figure 6. Correlations of between relative abundance (RA) of *Phocaeicola* and densities of tumor infiltrating lymphocytes (TIL) (A, B), tumor associated macrophages (TAM) (D, E) as well as the ratios of CD8(+) /CD3(+) (C) and CD163(+) /CD68(+) (F). Correlation coefficients (r) and p-values were calculated using Spearman's rank correlation coefficient. HPF= High power field

T-cell differentiation, or AhR altered macrophage polarization[29]. The extent to which *Phocaeicola* is involved in Tryptophan metabolism is unclear in this study, but analysis of amino acid metabolites may be useful to investigate its effects on immune cells around tumors. It also remains unclear why the RA of *Phocaeicola* was significantly lower in patients with nodal involvement than those without nodal metastases and significantly lower in tumors with distant metastases. It may be a passive phenomenon caused by tumor progression. However, this seems somewhat unlikely because the RAs of *Phocaeicola* did not have an association with tumor size or depth of invasion. Environmental changes around tumor due to dietary components or metabolites of intestinal bacteria could be affecting the phenomenon.

Recent taxonomic changes have resulted in some of the genus *Bacteroides* being placed in the genus *Phocaeicola*[9]. Among them *P. vulgatus* and *P. dorei* and others were previously classified as *Bacteroides.* In patients with coronary artery disease, significantly lower levels of *P. vulgatus* and *P. dorei* were detected[10,11]. It has also been shown that *P. vulgatus* may help prevent coronary artery disease by reducing gut microbial lipopolysaccharide[11]. Thus, it is becoming clear that *P. vulgatus* plays an important role in disease control. With respect to CRC, an increase in *Proteus mirabilis* and a decrease in *P. vulgatus* plays an important role in liver metastasis in CRC, which may be related to a decrease in Kupffer Cells in the liver[30]. Moreover, it is recently reported that *P. vulgatus* produces an Alpha-galactosylceramide (αGal-Cer) structure that can activate invariant natural killer T cells (iNKT) and the presence of *P. vulgatus* correlates with improved survival[31]. These facts raise a possibility that *P. vulgatus* may locally evoke cell-mediated immunity and suppress the progression of CRC. Although the species-level analysis in this study did not show significant differences due to the small number of samples, *P. vulgatus* shows a similar trend to *Phocaeicola genus* and may be one of the species to watch in the future (Supplementary Figure S1).

To the best of our knowledge, this is the first report to show an association between the abundance of *Phocaeicola* and metastatic status of CRC and suggests that *Phocaeicola* may affect the immune cell composition infiltrating CRC

tissue. The present study is limited by the small sample size of distal CRC. Therefore, the observed association may be a passive phenomenon caused by tumor progression. However, this seems somewhat unlikely because the RAs of *Phocaeicola* did not have an association with tumor size or depth of invasion. Taken together, the relative reduction of *Phocaeicola* in tumor tissue may lead to an immune microenvironment preferable for the development of tumor metastases. Mucosa associated microbiota may constitute an immune microenvironment which is critically related to tumor progression in CRC. Additional studies with a larger cohort are warranted.

Acknowledgements

We greatly appreciate Dr. Makiko Mieno for her supervision of statistical trend analyses and Prof. Adam Lebowitz for his English proofreading.

Conflicts of Interest

There are no conflicts of interest.

Author Contributions

Conceptualization: Gaku Ota, Hisanaga Horie, Yoshihiko Kono, Ryo Inoue, Joji Kitayama, Naohiro Sata; Methodology: Akira Saito, Ryo Inoue; Formal analysis: Ryo Inoue, Gaku Ota, Akira Saito; Writing-original draft preparation: Gaku Ota, Ryo Inoue, Hisanaga Horie; Writing-critical review and editing: Joji Kitayama, Naohiro Sata.

Approval by Institutional Review Board (IRB)

This study was approved by the ethics committee of Jichi Medical University Hospital (approval number: A17-083) and was conducted in accordance with the guiding principles of the Declaration of Helsinki, and written informed consent was obtained from each patient before inclusion in the study.

This manuscript is in accordance with your company's Ethics and Integrity Policy.

References

1. Ahn J, Sinha R, Pei Z, et al. Human gut microbiome and risk for colorectal cancer. J Natl Cancer Inst. 2013 Dec; 105(24): 1907-11.
2. Zeller G, Tap J, Voigt AY, et al. Potential of fecal microbiota for early-stage detection of colorectal cancer. Mol Syst Biol. 2014 Nov; 10(11): 766.
3. Yu J, Feng Q, Wong SH, et al. Metagenomic analysis of faecal microbiome as a tool towards targeted non-invasive biomarkers for colorectal cancer. Gut. 2017 Jan; 66(1): 70-8.
4. Wirbel J, Pyl PT, Kartal E, et al. Meta-analysis of fecal metagenomes reveals global microbial signatures that are specific for colorectal cancer. Nat Med. 2019 Apr; 25(4): 679-89.
5. Yachida S, Mizutani S, Shiroma H, et al. Metagenomic and metabolomic analyses reveal distinct stage-specific phenotypes of the gut microbiota in colorectal cancer. Nat Med. 2019 Jun; 25(6): 968-76.
6. Osman MA, Neoh HM, Ab Mutalib NS, et al. Parvimonas micra, Peptostreptococcus stomatis, Fusobacterium nucleatum and Akkermansia muciniphila as a four-bacteria biomarker panel of colorectal cancer. Sci Rep. 2021 Feb; 11(1): 2925.
7. Shah MS, DeSantis TZ, Weinmaier T, et al. Leveraging sequence-based faecal microbial community survey data to identify a composite biomarker for colorectal cancer. Gut. 2018 May; 67(5): 882-91.
8. Kono Y, Inoue R, Teratani T, et al. The Regional Specificity of Mucosa-Associated Microbiota in Patients with Distal Colorectal Cancer. Digestion. 2022; 103(2): 141-9.
9. García-López M, Meier-Kolthoff JP, Tindall BJ, et al. Analysis of 1,000 Type-Strain Genomes Improves Taxonomic Classification of Bacteroidetes. Front Microbiol. 2019 Sep; 10: 2083.
10. Emoto T, Yamashita T, Kobayashi T, et al. Characterization of gut microbiota profiles in coronary artery disease patients using data mining analysis of terminal restriction fragment length polymorphism: gut microbiota could be a diagnostic marker of coronary artery disease. Heart Vessels. 2017 Jan; 32(1): 39-46.
11. Yoshida N, Emoto T, Yamashita T, et al. Bacteroides vulgatus and Bacteroides dorei Reduce Gut Microbial Lipopolysaccharide Production and Inhibit Atherosclerosis. Circulation. 2018 Nov; 138 (22): 2486-98.
12. Thorsson V, Gibbs DL, Brown SD, et al. The Immune Landscape of Cancer. Immunity. 2018 Apr; 48(4): 812-30.e14.
13. Kitamura T, Qian BZ, Pollard JW. Immune cell promotion of metastasis. Nat Rev Immunol. 2015 Feb; 15(2): 73-86.
14. Pagès F, Mlecnik B, Marliot F, et al. International validation of the consensus Immunoscore for the classification of colon cancer: a prognostic and accuracy study. Lancet. 2018 May; 391(10135): 2128-39.
15. Zhou C, Liu Q, Xiang Y, et al. Role of the tumor immune microenvironment in tumor immunotherapy. Oncol Lett. 2022 Feb; 23(2): 53.
16. Galon J, Costes A, Sanchez-Cabo F, et al. Type, density, and location of immune cells within human colorectal tumors predict clinical outcome. Science. 2006 Sep; 313(5795): 1960-4.
17. Idos GE, Kwok J, Bonthala N, et al. The Prognostic Implications of Tumor Infiltrating Lymphocytes in Colorectal Cancer: A Systematic Review and Meta-Analysis. Sci Rep. 2020 Feb; 10(1): 3360.
18. Sica A, Larghi P, Mancino A, et al. Macrophage polarization in tumour progression. Semin Cancer Biol. 2008 Oct; 18(5): 349-55.
19. Matsumoto M, Inoue R, Tsuruta T, et al. Long-term oral administration of cows' milk improves insulin sensitivity in rats fed a high-sucrose diet. Br J Nutr. 2009 Nov; 102(9): 1324-33.
20. Inoue R, Ohue-Kitano R, Tsukahara T, et al. Prediction of functional profiles of gut microbiota from 16S rRNA metagenomic data provides a more robust evaluation of gut dysbiosis occurring in Japanese type 2 diabetic patients. J Clin Biochem Nutr. 2017 Nov; 61(3): 217-21.
21. Callahan BJ, McMurdie PJ, Rosen MJ, et al. DADA2: High-resolution sample inference from Illumina amplicon data. Nat Methods. 2016 Jul; 13(7): 581-3.
22. Bolyen E, Rideout JR, Dillon MR, et al. Reproducible, interactive, scalable and extensible microbiome data science using QIIME 2. Nat Biotechnol. 2019 Aug; 37(8): 852-7.
23. McDonald D, Jiang Y, Balaban M, et al. Greengenes2 unifies mi-

crobial data in a single reference tree. Nat Biotechnol. 2024; 42: 715-8.

24. Kong JC, Guerra GR, Pham T, et al. Prognostic Impact of Tumor-Infiltrating Lymphocytes in Primary and Metastatic Colorectal Cancer: A Systematic Review and Meta-analysis. Dis Colon Rectum. 2019 Apr; 62(4): 498-508.

25. Elliott LA, Doherty GA, Sheahan K, et al. Human Tumor-Infiltrating Myeloid Cells: Phenotypic and Functional Diversity. Front Immunol. 2017 Feb; 8: 86.

26. Camus M, Tosolini M, Mlecnik B, et al. Coordination of intratumoral immune reaction and human colorectal cancer recurrence. Cancer Res. 2009 Mar; 69(6): 2685-93.

27. Bai Z, Zhou Y, Ye Z, et al. Tumor-infiltrating Lymphocytes in Colorectal Cancer: The Fundamental Indication and Application on Immunotherapy. Front Imminol. 2022 Jan; 12: 80894.

28. Hezaveh K, Shinde RS, Klötgen A, et al. Tryptophan-derived microbial metabolites activate the aryl hydrocarbon receptor in tumor-associated macrophages to suppress anti-tumor immunity. Immunity. 2022 Feb; 55(2): 324-40.e8.

29. Xue P, Fu J, Zhou Y. The Aryl Hydrocarbon Receptor and Tumor Immunity. Front Immunol. 2018 Feb; 9: 286.

30. Yuan N, Li X, Wang M, et al. Gut Microbiota Alteration Influences Colorectal Cancer Metastasis to the Liver by Remodeling the Liver Immune Microenvironment. Gut Liver. 2022 Jul; 16(4): 575-88.

31. Ustjanzew A, Sencio V, Trottein F, et al. Interaction between Bacteria and the Immune System for Cancer Immunotherapy: The α-GalCer Alliance. Int J Mol Sci. 2022 May; 23(11): 5896.

Supplementary Files

Supplementary Figure S1. A Correlations of relative abundance (RA) of *Phocaeicola vulgatus* with pT stage (a), tumor diameter (b), pN stage (c), and pM stage (d). Differences among pT stage were analyzed using the Kruskal-Wallis test and between pN and pM stages using the Mann-Whitney U-test. N: lymph node metastases, M: distant metastases. Correlations with tumor size was evaluated with Spearman's rank correlation coefficients tests. B Correlations of between relative abundance (RA) of *Phocaeicola vulgatus* and densities of tumor infiltrating lymphocytes (TIL) (a, b), tumor associated macrophages (TAM) (d, e) as well as the ratios of CD8(+)/CD3(+) (c) and CD163(+)/CD68(+) (f). Correlation coefficients (r) and p-values were calculated using Spearman's rank correlation coefficient. HPF= High power field

Please find supplementary file(s);
http://dx.doi.org/10.23922/jarc.2024-014